Interlaminar crack initiation and growth rate in a carbon-fibre epoxy composite under mode I fatigue loading

A. Argüelles, J. Viña, A.F. Canteli, M.A. Castrillo, J. Bonhomme

Interlaminar crack initiation and growth rate in a carbon-fibre epoxy composite under mode I fatigue loading

A. Argüelles, J. Viña, A.F. Canteli, M.A. Castrillo, J. Bonhomme

PII: S0266-3538(07)00365-X
DOI: 10.1016/j.compscitech.2007.09.012
Reference: CSTE 3836

To appear in: *Composites Science and Technology*

Received Date: 2 May 2007
Revised Date: 17 September 2007
Accepted Date: 24 September 2007

Please cite this article as: Argüelles, A., Viña, J., Canteli, A.F., Castrillo, M.A., Bonhomme, J., Interlaminar crack initiation and growth rate in a carbon-fibre epoxy composite under mode I fatigue loading, *Composites Science and Technology* (2007), doi: 10.1016/j.compscitech.2007.09.012

Interlaminar crack initiation and growth rate in a carbon-fibre epoxy composite under mode I fatigue loading

Argüelles, A.[1], Viña, J.[2*], Canteli, A.F.[1], Castrillo, M. A.[1], Bonhomme, J.[3]

[1] Department of Construction and Manufacturing Engineering, University of Oviedo, 33203 Gijón, Spain

[2] Department of Materials Science and Metallurgical Engineering, Universidad de Oviedo, 33203 Gijón, Spain.

[3] ITMA Foundation Non Metallic Materials Technology Center, 33428 Llanera, Spain.

Abstract:

In this paper, interlaminar crack initiation and propagation under mode-I loading of a composite material made of an epoxy matrix reinforced with unidirectional carbon fibres are experimentally assessed for different asymmetry ratios. In the experimental program, DCB specimens were tested and the number of cycles to failure necessary for the onset of crack growth was registered for the asymmetry ratios R=0.2 and R=0.5. The G-N curves under fatigue loading were determined, N being the number of cycles at which delamination commences for a given energy release rate. The ΔG-da/dN curves associated with the previously generated crack growth were also determined for different G_{cr} rates (90%, 80%, 70%, etc.) and two different asymmetry ratios.

For the asymmetry ratios, the fatigue limits show values in the order of 50% and 70%, respectively, of the critical fracture energy resulting from the static tests employing the Modified Beam Theory. The fatigue limit is discretionally taken as the fatigue strength corresponding to 2.5 million cycles, i.e., the limit number of cycles considered for testing. The micrographs show that the morphology of the fracture toughness under mode-I loading are quantitatively but not qualitatively influenced by the stress ratios.

Keywords: Delamination, fatigue, fracture, composite material

* Corresponding author: jaure@uniovi.es

1. INTRODUCTION

Composites made of laminates exhibit a worrying susceptibility to the appearance and growth of cracks between the layers. This phenomenon, known as delamination, represents one of the most life-limiting failure modes of laminated composites. Delamination can be caused either by defects induced during the manufacturing process or generated in the structural elements during the service life of the material due to interlaminar stresses that can lead to the commencement of delamination. Additionally, delamination growth generally results in a loss of resistance and stiffness in the structural members leading to failure of the structure. Although several decades have elapsed since the recognition of the importance of interlaminar failure [1, 2], it still remains a determining factor limiting the use of structural elements made of laminated composites [3]. In recent years, a number of research projects have been conducted that focus on the determination of the characteristics of interlaminar failure under static loading [4-6]. However, new developments, predominantly in the aerospace field, compel us to complete the information on the behaviour of these materials with regard to delamination under varying loading conditions [7-12]. In this study, the initiation and propagation of interlaminar cracks under mode-I cycling loading is experimentally investigated using a composite made of unidirectional carbon fibre with an epoxy matrix, varying the asymmetry coefficient.

2. EXPERIMENTAL PROCEDURE.

2.1 Materials and specimens.

The composite material employed in this research program was manufactured from Hexcel AS4/8552 RC34 AW196 epoxy resin prepregs, reinforced with unidirectional carbon fibre AS4 sequentially piled and cured in an autoclave, resulting in a volume fraction of 60% . The laminate configuration consists of 16 plies with 0º orientation /insert/ 16 plies with 0º orientation, employing an RF-260-R Tygavac 20 micrometer thick insert film. Seven specimens were tested in accordance with ASTM D3039 for the static characterization of the material under tension and according to ASTM D3518 for static characterization under shear providing the following results:

Young moduli

E_{11}: 144 GPa (C.V.: 7.8%)

E_{22}: 10.6 GPa (C.V.:5.9%)

Ultimate stress:

σ_{11}: 1703 MPa (C.V.: 9.2%)

σ_{22}: 30.8 MPa (C.V.:11%)

Shear modulus:

G_{12}: 5.36 GPa (C.V.:12%)

Shear ultimate stress:

$\tau_{máx}$: 67.7 MPa (C.V.:1.6%)

where sub-index 11 denotes fibre orientation and 22, the direction perpendicular to the fibres. The specimens were obtained from panels manufactured by cutting the laminates. A double cantilever beam (DCB) was used to characterize delamination under mode-I conditions for both static and cyclic loading. Figure 1 shows the geometry of the specimen used in accordance with ASTM in which a non-adhesive insert is placed midplane to provoke the initial delamination. Two hinges are glued, respectively, to the edge of both specimen legs, thus allowing the external load to be applied.

Figure 1.

2.2 Static and fatigue characterization.

All the tests performed to characterize the material both under static and cyclic loading were carried out in a servo-hydraulic MTS testing machine provided with a 5kN load cell controlled by a computer using the original software. For the calculation of the static fracture toughness of the material, three methods were applied in accordance with the ASTM D5528 Standard [13]: the Modified Beam Method (MBT), the Compliance Calibration Method (CC) and the Modified Compliance Calibration Method (MCC). A deformation rate of 0.5 mm/min was applied throughout the tests [14]. The experimental results obtained for the static fracture toughness G_c according to the three methods are summarized in Table 1 showing an acceptable agreement:

Table 1.

The aim of the fatigue tests was to provide information on the material to be used in the fatigue life prediction of laminates. This objective was twofold:

a) To find out the number of cycles needed to initiate delamination for a given energy release rate, i.e., to determine the fatigue curves ΔG-N.
b) To characterize the propagation phase by means of the crack growth curve da/dN-ΔG.

In order to reasonably extend the test duration without implying a pronounced increase in costs, tests were conducted up to 2.5 million instead of the 2 million cycles usually considered as a standard number of fatigue limit cycles .

a) ΔG-N fatigue curves

In the present study, delamination growth onset was decided by visual observation of the crack opening at the crack front. This procedure is in agreement with one of the three alternatives suggested by the ASTM D6115 standard [15] to determine the number of cycles until the onset of delamination though the method based on compliance increase is recommended as being more conservative under load control conditions. At this moment, the crack is ideally assumed to be initiated, though not having developed. This is repeated for different ΔG values, thus allowing the fatigue curve $\Delta G_c(N)$ to be plotted. The procedure is similar to that applied for the conventional test to determine S-N curves. Two asymmetry coefficients R=0.2 and R=0.5 were here employed. In all cases, the maximum stress was maintained constant and the minimum stress was varied as a function of the adopted asymmetry coefficient [9].

b) da/dN-ΔG crack growth rate curves

The crack growth rate, i.e., the da/dN- ΔG curves, were determined for a fraction of the critical energy release rate G_{crit} (80%) and for different $R=\delta_{min}/\delta_{max}$ relations[14]. A frequency of 3 Hz was applied throughout the tests.

Although it is difficult and cumbersome to perform the test, it seems to be an effective way of obtaining valid information. The same asymmetry coefficients were used here as in the study of crack initiation, i.e., 0.2 and 0.5.

Since the aim of the tests is to gain knowledge about the onset of delamination and to determine the crack growth rate, they were all carried out under displacement control, contrary to usual fatigue tests, which are generally conducted under load control. This is due to the fact that, under load control, increasing stress arises at the crack front during its progression, thus causing crack instability of the specimen when the crack reaches a certain value, unless constant stress may be ensured at the crack tip via steady load variation. This means applying appropriate load control of the real crack length in the machine under consideration. The procedure employed consisted in controlling the displacement, i.e., the crack opening displacement, via the critical displacement obtained from the static characterization of the material.

By adjusting this displacement as the crack grows, it is possible to keep the stress state constant at the crack front throughout the test. The crack length values were read by means of a 100x portable microscope, located at one side of the specimen.

The test was stopped after every 10^4 cycles in order to determine the crack length and thus crack growth rate by optical observation without removing the specimen from the fixture. The mean load was applied while locating the crack front under the microscope and measuring crack growth. In this way, the crack growth rate da/dN was calculated. The energy release rate for the last 10^4 cycles was evaluated using the mean values of the crack length and the maximum and minimum loads.

3. EXPERIMENTALS RESULTS.

In the following, the experimental results obtained from the tests are presented.

3.1 Beginning of delamination.

Figure 2 represents the curves characterizing the fatigue behaviour of the material (crack growth onset) for the two asymmetry coefficients considered in the tests.

Figure 2.

The values of the critical energy obtained from the tests are represented as a percentage. A reference fatigue limit, discretionally taken as the fatigue strength for 2.5 million cycles, i.e., the limit number of cycles, corresponds to approximately 50% of the critical fracture energy calculated from the static tests according to the Modified Beam Method for an asymmetry coefficient of 0.2, and to around 70% for an asymmetry coefficient of 0.5.

The pronounced scatter observed by the results of the number of cycles elapsed until crack initiation could presumably be assigned to the strip of resin accumulated at the crack front as a result of the manufacturing process and to the 20 micrometer thickness of the insert film, which exceeds the 13 micrometer prescribed by ASTM D5528.

3.2 Delamination crack rate.

Figures 3 and 4 show the crack growth rate as a function of the crack length for the tested material for a loading level corresponding to 80% of the critical delamination energy and asymmetry coefficients of 0.5 and 0.2, respectively.

Figure 3.

Figure 4.

As can be observed, the growth rate slows down with increasing crack length. For better understanding of the process, Figure 5 shows both curves on the same graph for the same crack length. Although the overall behaviour is similar in both cases, significant differences arise. The crack growth rate becomes higher for crack lengths less than 4 mm. For crack lengths over this value, crack progression decreases, practically ceasing to grow for crack lengths over 10 mm and an asymmetry coefficient equal to 0.5 stops. It should be remembered that the maximum stress level was kept constant for both asymmetry coefficients, only the minimum stress being changed.

The crack growth rate increases for an asymmetry coefficient of 0.2, varying around $1.5 \cdot 10^{-4}$ mm/cycle, while for an asymmetry coefficient of 0.5, the growth rate varies around $1.64 \cdot 10^{-4}$ mm/cycle during the first 10 mm of crack length.

Figure 5.

Figure 6 represents the crack growth rate under fatigue loading as a function of the increase in the critical delamination energy, calculated using the Modified Beam Theory, for the two asymmetry coefficients considered in this study and a mean load level corresponding to 80% of the critical energy associated with static fracture of the material.

Figure 6.

In this same figure, a certain pattern of behaviour is observed, which is practically coincident for both cases, showing the same trend in crack growth, the highest crack growth rates corresponding to the increases in critical energy.

In Figure 7, the crack growth rate is represented as a function of critical delamination for an asymmetry coefficient energy of 0.5 and load levels of 80, 85 and 90% of the critical delamination energy of the material under static load.

Figure 7.

In this case, lower crack growth rates are obtained with decreasing load levels, presenting mean rates of $4.71 \cdot 10^{-5}$ mm/cycle, $6.99 \cdot 10^{-5}$ mm/cycle and $7.44 \cdot 10^{-5}$ mm/cycle for 80%, 85% and 90% ΔG, respectively, and crack lengths close to 20 mm.

3.3 Fracture surfaces

Figure 8 depicts a number of fracture surfaces of one of the specimen tested under a stress ratio R=0.2. Micrograph [a] represents the transition zone between the insert initiating delamination and the crack front at a magnification of 1000x. In [b], the crack growth zone of the same specimen is shown under the same magnification as before. In [c], the fracture surface of the same specimen zone is represented at the same scale, this time for another crack, which is markedly longer. Finally, a detail of the fibre failure mode in the crack growth zone is shown at a magnification of 4000x.

Figure 8.

Figure 9 shows different fracture surface zones in another specimen tested under a stress ratio R= 0.5. Micrographs [a] and [d] depict the same zones as those referred to previously in Figure 8.

Figure 9.

As regards the morphology of the fracture surface of the laminate under mode-I cyclic load, a certain difference between the generated fracture surfaces is observed when the stress ratio is changed. This becomes apparent when observing the higher degree of damage of the matrix-fibre interface occurring in the specimen tested at a higher stress level R = 0.2. Here, a certain separation between fibres and matrix is observed (see Figures 8 a) and c)) both in the initiation and in the growth zones. However, in the material subjected to a lower stress range, R=0.5, less separation and debonding of fibres is observed.

In the case of the higher stress level, the trajectories of the cracks generated were found to be mainly oriented along the interface fibre-matrix. Another important difference between the two fracture surfaces is found in the striation appearing in the resin. This effect is more noticeable in the case of the material subjected to a lower stress level, which could be explained by the presence of a lower propagation velocity at an overall level, since the fracture surface developed is broader.

4. CONCLUSIONS.

In this paper, certain parameters controlling the delamination process of a composite under mode-I fatigue loading were experimentally investigated. The results may be summarized as follows:

- As regards interlaminar crack initiation:

The determination of the fatigue curves was strongly influenced by the process of manufacturing the laminate, the accumulation of resin at the crack front and possibly by the film thickness, which led to pronounced variability in the data. As a consequence, the study and interpretation of the influence of these parameters requires the testing of a large number of specimens.

Fatigue fracture under mode-I loading may be characterized by carrying out the tests under displacement control, i.e., by regulating the opening of the crack lips as a function of the critical displacement obtained from the static characterization. The fatigue versus asymmetry coefficient curves show the expected behaviour, i.e., a higher fatigue limit with decreasing stress range.

- As regards crack growth:

Crack growth slows down with increasing crack lengths and can even stop progressing if the critical fracture energy supplied does not exceed the equivalent values calculated from the static characterization of the material. This could be due to the increasing compliance of the crack legs under cyclic loading caused by viscoelastic effects or to fibre bridging at the crack as evidenced by the R-curve of the material.

With increasing stress range, a decreasing crack growth rate was observed during the tests, which could once more be assigned to the increasing compliance of the specimen legs.

5. ACKNOWLEDGEMENTS

The authors are indebted to the Spanish Ministry of Science and Technology (Project MAT2003-09768-C03-03) for partial funding of this work.

6. REFERENCES.

[1] O'Brien TK., Characterization of delamination onset and growth in a composite laminate. In: Reifsnider KL, editor. Damage in Composite Materials, ASTM STP 775, (1982) 140-167.

[2] Standard tests for toughened resin composites. NASA RP 1092; (1983).

[3] Paul D, Kelly L, Venkayya V, Hess T., Evolution of U.S. military aircraft structures technology. J Aircraft 39(1), (2002) 18-29.

[4] Hojo M., Matsuda S., Tanaka M, Göran Gustafson C., Hayashi R., Effect of stress ratio on near-threshold propagation of delamination fatigue cracks in unidirectional CFRP, Composites Science and Technology 29, (1987) 273-292.

[5] Hansen U., Gillespie, J. W., Dependence of intralaminar fracture toughness on direction of crack propagation in unidirectional composites. Journal of Composites Technology & Research, 20, (1998) 89-99

[6] Brunner A.J., Experimental aspects of Mode I and Mode II fracture toughness testing of fibre-reinforced polymer-matrix composites. Computer Methods Applied Mechanics Engineering 185 (2000) 161-172.

[7] Ashcroft, I. A., Hughes, D. J., and Shaw, S. J., Mode I Fracture of Epoxy Bonded Composite Joints: 1. Quasi-Static Loading, Int. J. Adhesion and. Adhesives, 21. (2001) 87–99.

[8] Hojo M., Ando T., Tanaka M., Adachi T., Ochiai S., Endo Y., Modes I and II interlaminar fracture toughness and fatigue delamination of CF/epoxy laminates with self-same epoxy interleaf. International Journal of Fatigue 28 (2006) 1154–1165.

[9] Kunigal Shivakumar, Huanchun Chen, Felix Abali, Dy Le, Curtis Davis. A total fatigue life model for mode I delaminated composite laminates. International Journal of Fatigue 28 (2006) 33–42

[10] Mahdi S. , Kim H. J.. Gama B. A. Yarlagadda S. Gillespie J. W. A Comparison of Oven-cured and Induction-cured Adhesively Bonded Composite Joints, Journal of composite materials, 37(6) (2003) 519-542

[11] Matsubara G., Ono H., Tanaka K., Mode II fatigue crack growth from delamination in unidirectional tape and satin-woven fabric laminates of high strength GFRP, International Journal of Fatigue 28 (2006) 1177–1186.

[12] Pizhong Qiao, Guanyu Hu, Mode-II Fatigue Fracture of Wood–Composite Bonded Interfaces. Journal of Composite Materials, Vol. 38, No. 6(2004), 453-473

[13] ASTM D 5528-01 Modo I Interlaminar fracture toughness of unidirectional fiber-reinforced polymer matrix composites

[14] Hojo M., Matsuda S., Tanaka M, Ochiai S., Murakami A., Mode I delamination fatigue properties of interlayer-toughened CF/epoxy laminates, Composites Science and Technology 66 (2006), 665-675.

[15] ASTM D 6115-97 Mode I fatigue delamination growth onset of unidirectional fiber-reinforced polymer matrix composites

List of captions:

Table 1. Fracture toughness obtained for the material used.

Figure 1. Specimen geometry, H_{mean}=9.22mm.

Figure 2. Fatigue curves for the material tested.

Figure 3. Propagation rate *versus* the crack length for an asymmetry coefficient of 0,5.

Figure 4. Propagation rate versus the crack length for an asymmetry coefficient 0,2.

Figure 5. Propagation rate versus crack length for asymmetry coefficients of 0,2 and 0,5.

Figure 6. Crack growth rate versus the increase in critical energy for different values of the asymmetry coefficient.

Figure 7. Crack growth rates for different increases in the critical delamination energy and an asymmetry coefficient of 0,5.

Figure 8. SEM micrographs of the material fracture surface for R = 0,2.

Figure 9. SEM micrographs of the material fracture surface for R = 0,5.

Fig.1

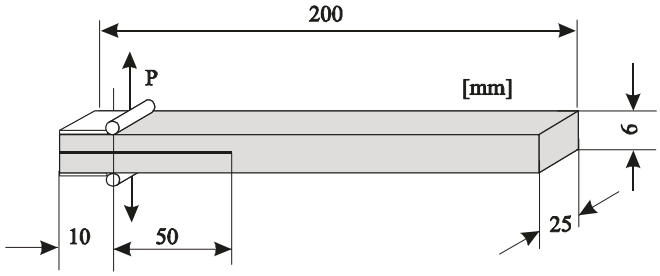

Fig.2

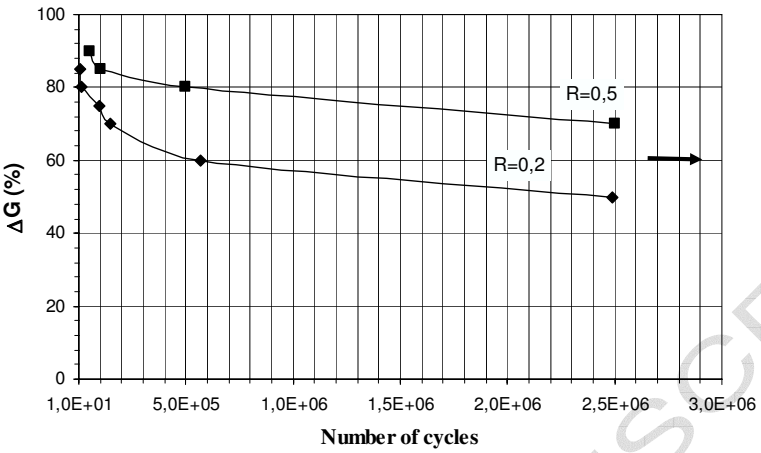

Fig.3

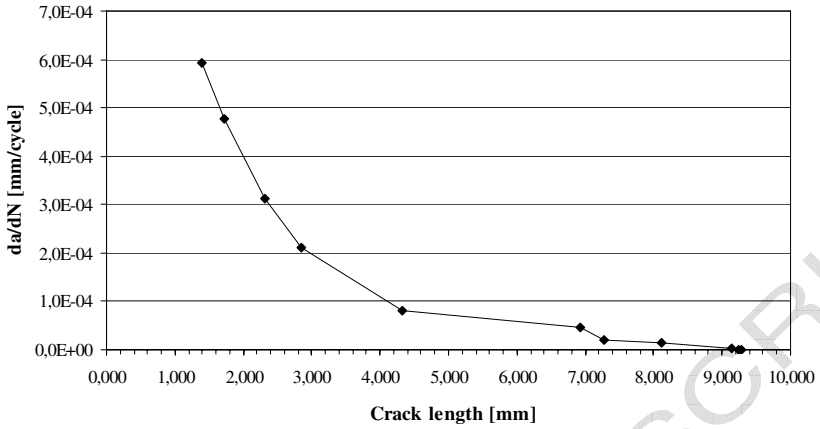

Fig.4

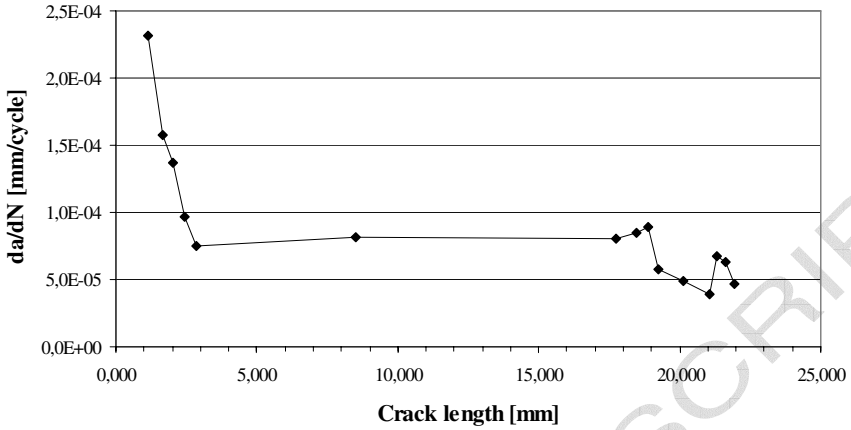

Fig.5

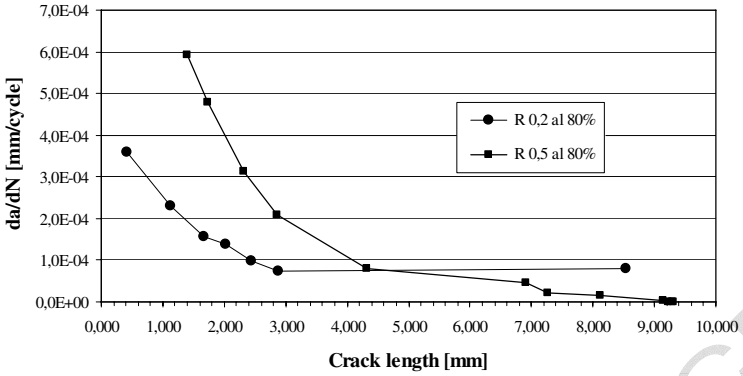

Fig.6

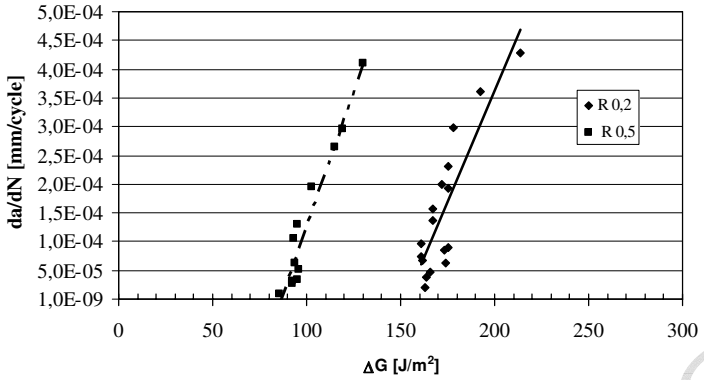

Fig.7

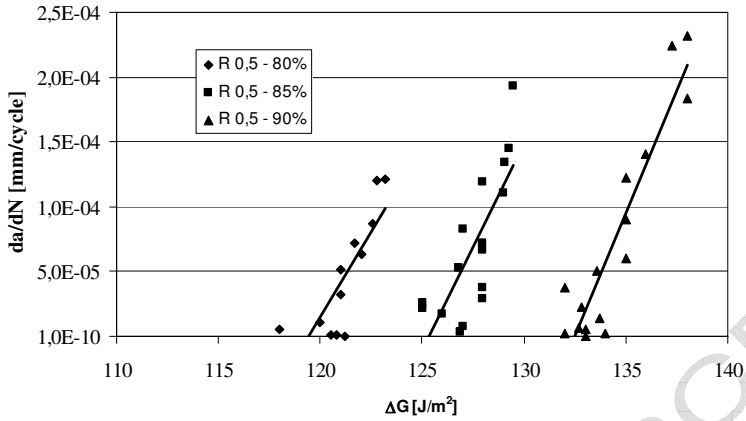

Fig.8

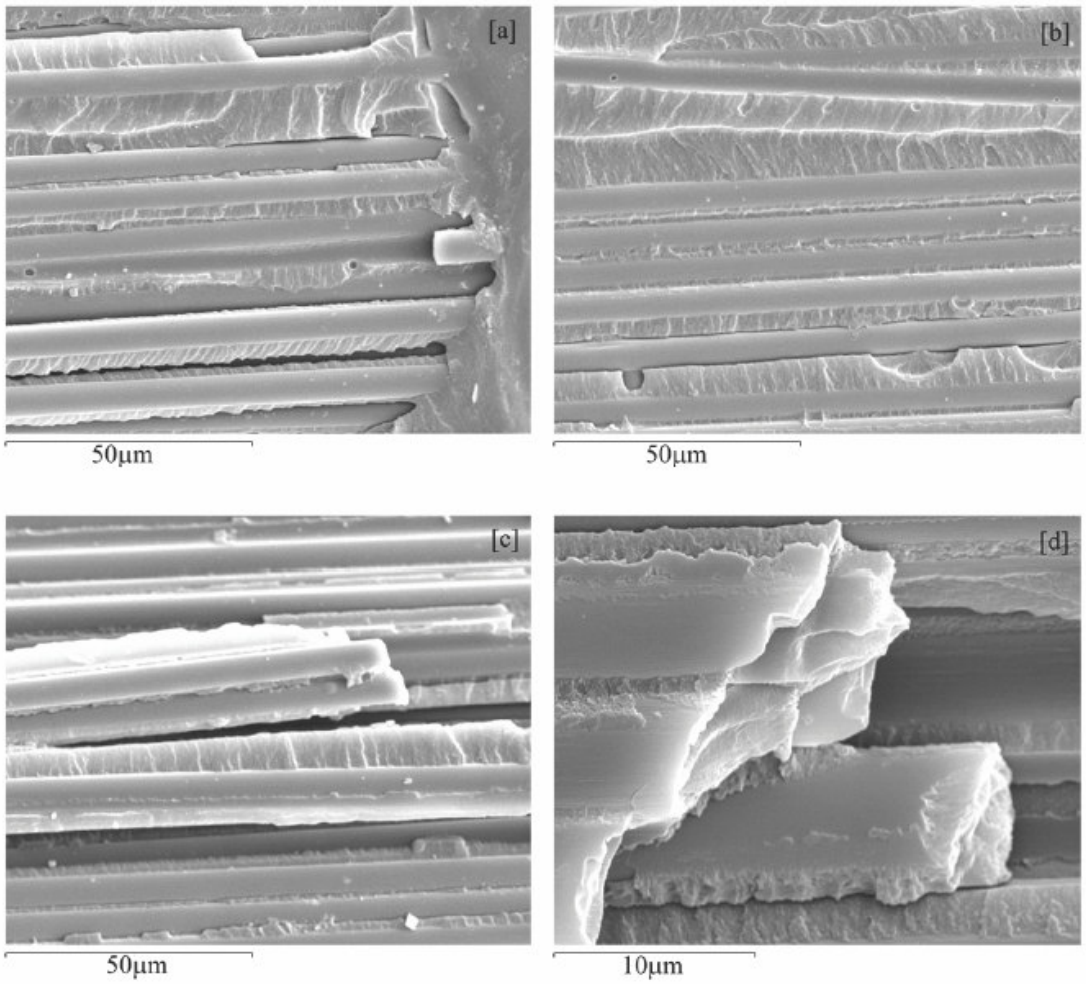

Fig.9

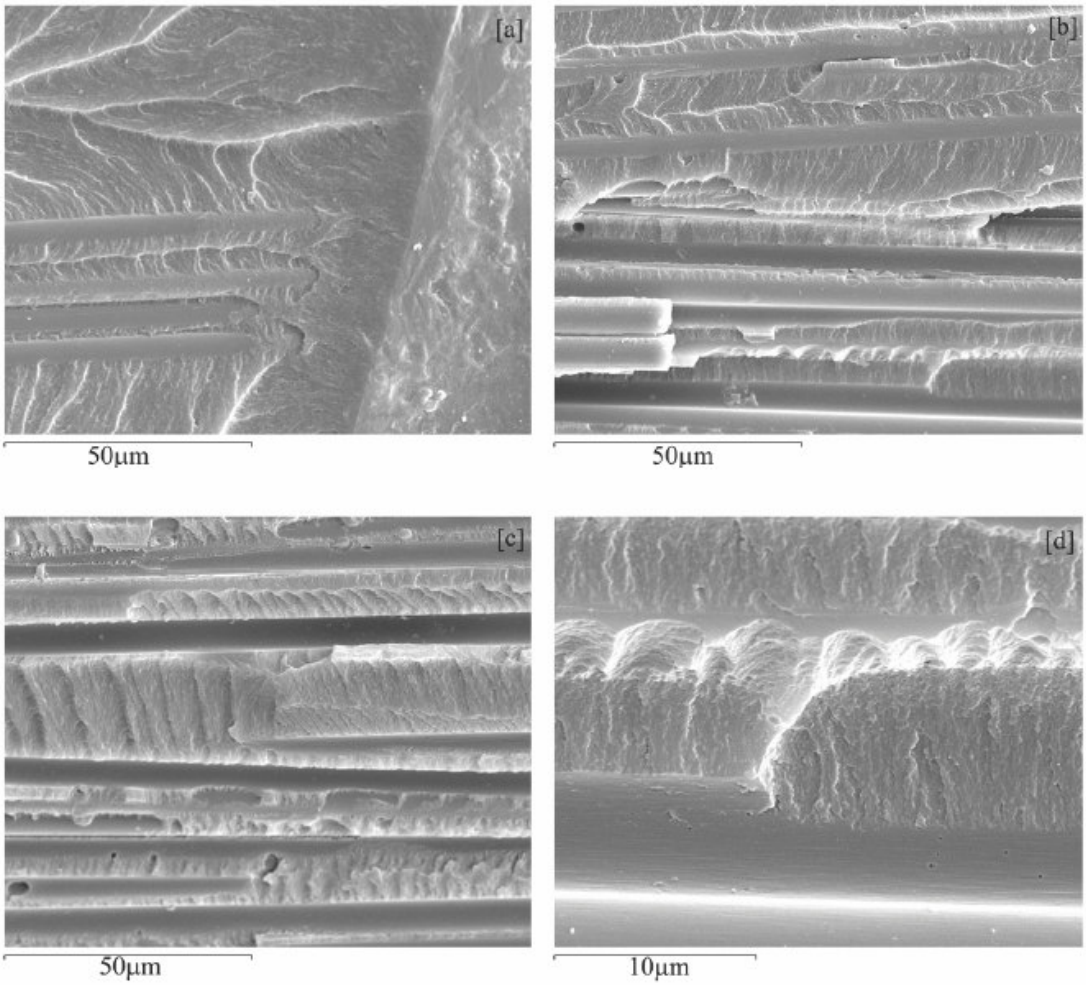

Table 1

	G_{Ic} [J/m^2] **(MBT)**	G_{Ic} [J/m^2] **(CC)**	G_{Ic} [J/m^2] **(MCC)**
Mean	302.105	319.531	298.082
Standard Deviation	29.155	39.382	35.666
Coefficient of Variation [%]	9.650	12.325	11.965